A New Current-Balancing Method for Paralleled LED Strings

Yuequan Hu and Milan M. Jovanović
Delta Products Corporation
Delta Power Electronics Laboratory
5101 Davis Drive, RTP, NC 27709, U.S.A.
Tel: (919) 767-3980, Fax: (919) 767-3967, Email: milan@deltartp.com

Abstract – This paper presents a current balancing and dimming scheme for paralleled light-emitting-diode (LED) strings directly powered by a dc source. The current balancing is achieved using current-balancing transformers. To make the operation of the balancing transformers possible and provide equal driving currents for the paralleled LED strings, a series-connected switch is turned on or off by a high-frequency signal. The brightness of the LED strings can be adjusted by varying the duty cycle of the control switch in addition to achieving current balancing. The proposed current-balancing and dimming method was verified experimentally.

I. INTRODUCTION

As mercury-free solid-state light sources with superior longevity and low-maintenance, LEDs are inevitably poised to replace existing lighting sources such as incandescent and fluorescent lamps in the future. Since a light-emitting diode (LED) is a semiconductor device that emits light when its p-n junction is forward biased and its brightness is directly related to the current flowing through the junction, an effective way to ensure that each LED produces similar light output is to connect them in series so that all LEDs in the string have the same current. A major drawback of a series connection of LEDs is the cumulative voltage drop that eventually limits the number of LEDs in a string. This limitation can be overcome by paralleling LEDs or LED strings. However, since the voltage-current characteristic (V-I curve) of individual LED differs and the LED's forward-voltage drop exhibits a negative temperature coefficient, paralleled LED strings may not have the same currents unless a current balancing mechanism is provided.

Generally, the current balancing of LED strings connected in parallel can be achieved by a number of techniques. In the simplest approach, shown in Fig. 1, current balancing is achieved by identical current-limiting resistors R_1 to R_n connected in series with each corresponding LED string. While this approach offers simplicity and low cost, its performance is very limited. Specifically, the current balancing accuracy of this passive method solely depends on the matching of the LED string voltages and tolerances of the current-limiting resistors. Generally, its current balancing performance is poor since LED string voltages exhibit significant differences primarily due to manufacturing tolerances and temperature variations. Moreover, this method suffers from significant power loss in the series resistors.

A method that offers a high current-balancing accuracy is shown in Fig. 2. In this method, the current in each LED string is independently regulated by a corresponding current regulator. As a result, the current in each string can be set precisely to the desired current. However, since this requires a current regulator for each string, its implementation cost is relatively high, especially in applications with a large number of paralleled LED strings. Generally, the current regulators in Fig. 2 can be of a linear [1]-[8] or switching type [9]-[13]. The switching regulators offer better efficiency than the linear regulators and can be implemented with a step-up and/or step-down topology making it possible to drive a variety of LED strings, including those with string voltages higher than the source voltage. While the linear current regulators cannot match the efficiency of the switching regulators and can only be employed to drive LED strings with a voltage lower than the supply voltage, they are more cost effective than their switching counterparts.

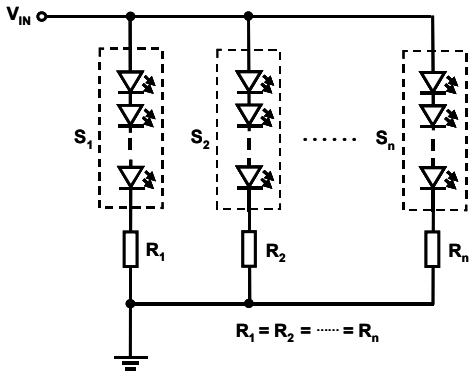

Fig. 1. Balancing driving-currents of paralleled LED strings using series resistors.

Methods that provide excellent current balancing with a reduced cost compared with the method in Fig. 2 were presented in [14]-[16]. A typical implementation of these

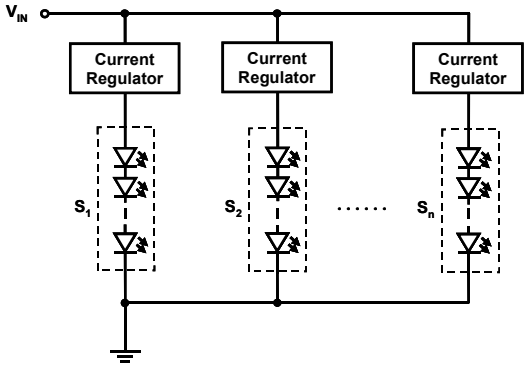

Fig. 2. Balancing driving-currents of paralleled LED strings using current regulators.

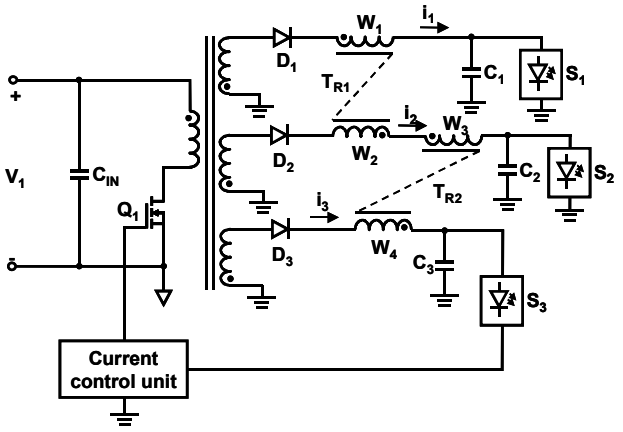

Fig. 3. Driver for paralleled LED strings with current balancing transformers.

methods that is shown in Fig. 3 employs current balancing transformers to equalize the currents of the LED strings. Two transformers with equal number of turns of the primary and secondary windings are connected between the output rectifier and the filtering capacitor. The current feedback from one output is used to set and regulate the current of the corresponding LED string. Because of the 1:1 turns ratio of the transformer windings, the current flowing through one winding of the transformer produces a current of the same magnitude in the other winding of the transformer provided that the magnetizing current of the transformer is small compared to the winding current. Because the two current-balancing transformers have their windings W_2 and W_3 connected in series, all three strings carry the same current.

The major deficiency of this cost-effective magnetic current balancer is that it needs to be integrated with a switch-mode power supply, i.e., it cannot be used independently. As a result, this approach lacks the flexibility to operate with an arbitrary dc source, for example, a dc battery. In addition, the integration of the magnetic balancer into a switch-mode power supply increases the complexity and, therefore, the cost of the power supply because it requires a separate output for each string. This is especially detrimental in applications with a large number of paralleled LED strings.

In this paper, a cost-effective and high-performance current balancer that can operate from any dc source is presented. The proposed method provides not only good current balancing but also high-frequency pulse-width-modulated (PWM) dimming for paralleled LED strings without any assistance from the dc source.

II. Proposed DC-Side Current Balancer Concept

The conceptual diagram of the proposed driver with a current balancer for paralleled LED strings is shown in Fig. 4. It consists of a power supply providing current i_O, a magnetic balancer with identical current-balancing transformers and control switch(es) each connected in series with a corresponding LED string. The power supply can be any type of power sources, e.g., an ac/dc or a dc/dc converter, or a battery. The control switch, which is periodically turned on and off, plays two roles. Its major role is to provide a flux-reset mechanism for the current-balancing transformers, i.e., to enable the operation of the transformer with a dc power source. Namely, during turn-on time of the switch, the current flows through the string connected to the switch, whereas during turn-off time of the switch, the current through the string is zero and the magnetic core of the transformer is reset. Because of the switching, the average current through the k^{th} LED string is $I_{AVE(k)} = i_k D$, where i_k is the current amplitude of k^{th} LED string (k = 1, 2, ·····, n), $D = T_{ON}/T_S$ is the duty cycle of the switch, T_{ON} is the turn-on time of control switches and T_S is the switching period. Since the brightness of the LEDs is directly related to the average driving current, the brightness of the LEDs can be varied by varying duty cycle D. Therefore, another function of the switch is to provide the PWM (pulse-width-modulated) dimming. However, it should be noted that dimming can also be achieved by changing the output voltage/current of the power supply, i.e., without the need for the PWM of the control switch in the current-balancing circuit. If the control switch in Fig. 4 is not used for dimming, its duty cycle should be maximized to provide the maximum possible brightness.

The LED string balancing circuit in Fig. 4 assumes that supply current i_O is regulated, i.e., that the power supply is a constant current source. However, the proposed LED-string current-balancing method can also be applied to LED strings supplied by a voltage source by adding resistor R_{CS} in series with switch Q_1, as shown in Fig. 5. For a given supply voltage V_O, the value of R_{CS} is selected so that the total current of LED strings S_1-S_n is set to the desired level. It should be noted that the power dissipation of resistor R_{CS} can be minimized by adjusting the current via current feedback, as shown by the dashed line in Fig. 5, i.e., by sensing the voltage across R_{CS} and changing supply voltage V_O to obtain the desired current. The addition of resistor R_{CS} has no effect on the operation of the current sharing circuit.

Generally, a magnetic current balancer can be implemented with various connections of current-balancing transformers [16]-[18]. The current balancing circuit shown in Fig. 5 employs a transformer for every two neighboring LED strings. The transformer windings are connected in such a way that the current of an LED string flows into a dotted end of one winding of the transformer while the current of the neighboring LED string flows out of a dotted end of the other winding of the same transformer. Because current-balancing transformers T_1-T_n have a unity turns ratio, i.e., equal number of the primary and secondary turns, their primary and secondary currents can be considered to be equal if the magnetizing current of the transformers is much smaller than the winding current. Therefore, in the circuit in Fig. 5, assuming that the magnetizing current is negligible, the primary current and secondary current of each transformer (T_1~T_{n-1}) are equal, resulting in equal string currents in the proposed current-balancing method, i.e., $i_1 = i_2 = i_3 = \cdots\cdots = i_n$, regardless of LED-string voltages.

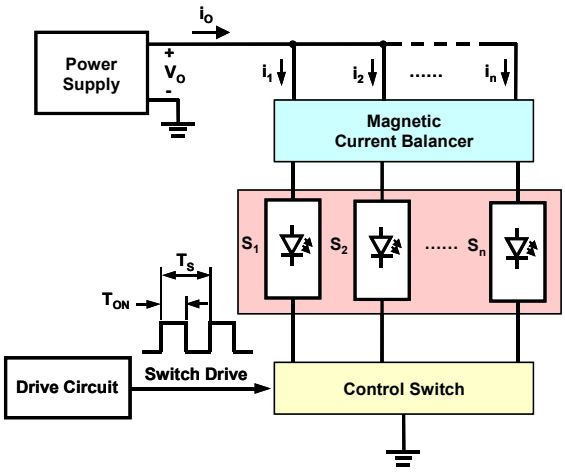

Fig. 4. Conceptual diagram of proposed driver with current balancer for paralleled LED strings.

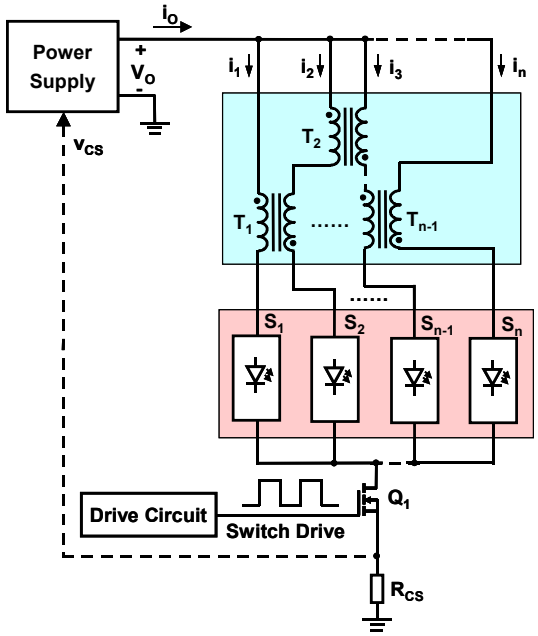

Fig. 5. Simplified implementation circuit of proposed current balancer.

III. ACCURACY ANALYSIS

In the proposed current-balancing circuit, the magnetizing current has the paramount effect on the current balancing (sharing) performance. To facilitate the understanding of the operation of the proposed current balancer and the evaluation of its current-balancing performance, the simplest current balancer with two paralleled LED strings, shown in Fig. 6 (a), is analyzed. In this analysis, each LED string is modeled by a series connection of an ideal diode D_S, equivalent dc voltage source V_S (equal to the turn-on threshold), and equivalent series resistance R_S, as well as total string capacitance C_S connected in parallel. When switch Q_1 is turned on, as shown in Fig. 6 (a), currents i_1 and i_2 flow through strings S_1 and S_2, respectively, and

$$v_1 + v_{S1} = V_O, \quad (1)$$
$$-v_2 + v_{S2} = V_O, \quad (2)$$
$$i_1 = i_2 + i_M, \quad (3)$$

where v_{S1} and v_{S2} are the voltages across the first and second strings, respectively.

Since $v_1 = v_2$ because of the unity turns ratio of the current-balancing transformer, from (1) and (2),

$$v_1 = v_2 = (v_{S2}-v_{S1})/2, \quad (4)$$

i.e., the voltage across the current-balancing transformer windings is the average of the string-voltage mismatch.

As can be seen from (3), the mismatch of string currents is equal to magnetizing current i_M. Assuming $v_{S2} > v_{S1}$, the increase of magnetizing current i_M during turn-on time of switch Q_1 is a function of primary-winding voltage v_1, duty cycle D, switching period T_S, and magnetizing inductance L_M, i.e.,

$$\Delta i_M = \frac{v_1 D T_S}{L_M} = \frac{(V_{S2} - V_{S1})D}{2 f_S L_M}. \quad (5)$$

When switch Q_1 is turned off, the string currents continue to flow charging drain-to-source capacitance C_{OSS} of the switch, as shown in Fig. 6 (b). The rising switch voltage decreases string currents i_1 and i_2, as well as their respective string voltages v_{S1} and v_{S2}. Eventually, the string with a higher forward voltage, e.g., string S_2, is turned off, and its string capacitance C_{S2} starts discharging by current i_2, as illustrated in Fig. 6(c). However, string S_1 that has a lower forward voltage stays on as long as magnetizing current i_M in Fig. 6(c) is larger than current i_2. In fact, the magnetizing current continues to increase until string voltage v_{S2} becomes equal to string voltage v_{S1}. After this moment, the transformer core starts to reset, i.e., magnetizing current i_M starts decreasing since $v_{S1}>v_{S2}$ and a negative voltage is applied across the magnetizing inductance L_M.

As derived in the Appendix, the peak magnetizing current $i_{M(pk)}$, which represents the upper limit of the mismatch of string currents is given by

$$i_{M(pk)} = \left(1 + \frac{\cos\frac{1-D}{f_S\sqrt{L_M C_{EQ}}}}{1-\cos\frac{1-D}{f_S\sqrt{L_M C_{EQ}}}} \right) \cdot \frac{(V_{S2} - V_{S1})D}{2 f_S L_M} \quad (6)$$

for

$$0 < \frac{1-D}{f_S\sqrt{L_M C_{EQ}}} \le \frac{\pi}{2}, \quad (7)$$

where $C_{EQ} = 4C_{S2} + C_{OSS}$.

It should be also noted that expression (6) can be applied with reasonable accuracy in the extended range given by

$$\frac{\pi}{2} < \frac{1-D}{f_S\sqrt{L_M C_{EQ}}} \le \pi. \quad (8)$$

From (6), it can be seen that the accuracy of the current sharing of the proposed method is a function of string-voltage

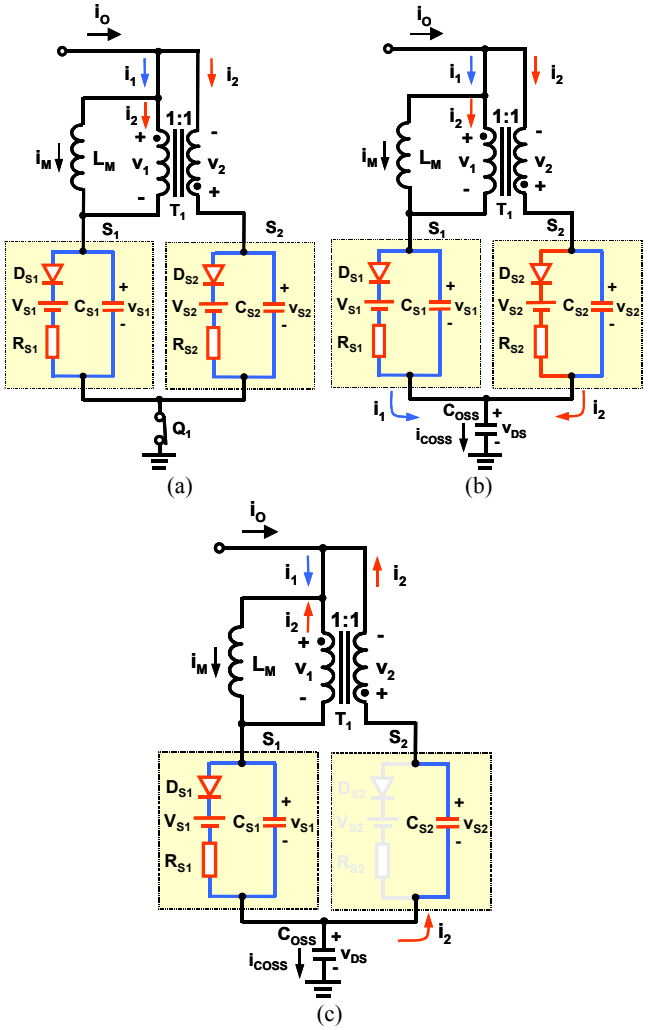

Fig. 6. Equivalent circuits of proposed current balancer for paralleled LED strings. (a) Switch Q_1 on; (b) switch Q_1 off and string S_2 still turned on; (c) both switch Q_1 and string S_2 turned off.

mismatching (V_{S2}-V_{S1}), duty cycle D, magnetizing inductance L_M, switching frequency f_S and capacitances C_{S2} and C_{OSS}.

IV. Design Considerations

Since both the current-balancing error and the average LED string current are proportional to duty cycle, the major design-optimization objective for the proposed driver is to provide current balancing between paralleled strings without limiting their ability to deliver the maximum rated light output. Therefore, the major design challenge is to keep the current balancing error small while maximizing the duty cycle D, i.e., operating with a duty cycle in the 85%-95% range. To facilitate the understanding of the effect of parameter value selection on the current-balancing performance, Figs. 7, 8, and 10 show plots of $i_M(pk)$ as a function of magnetizing inductance L_M, equivalent parasitic capacitance C_{EQ}, and switching frequency f_S, respectively. The plots are given for duty cycles 95%, 90%, 85%, and 75%, and for a range of parameter values expected in the majority of practical implementations. Moreover, because the plots are given for the string voltage mismatch (V_{S2}-V_{S1})=1V and since the peak magnetizing current according to (6) is a linear function of (V_{S2}-V_{S1}), the peak magnetizing current for any other voltage mismatch can be obtained by directly scaling the values in the plots by the value of the voltage mismatching expressed in Volts. Finally, it should be noted that the dashed segments of the lines in the figures represent the extended validity range of (6), as given by (8).

As can be seen from Fig. 7, for a given duty cycle in the 85% to 95% range, the peak magnetizing current and, therefore, the current balancing accuracy is virtually independent of the magnetizing inductance value as long as the magnetizing inductance is selected to be greater than approximately 2 mH. However, for a given duty cycle, the current-balancing accuracy is a strong function of the parasitic capacitances of the LED strings and the drain-to-source capacitance of switch Q_1, as illustrated in Fig. 8. To achieve a better accuracy, the capacitances need to be reduced. The reason for such a strong dependence of the magnetizing current on the parasitic capacitances can be explained by analyzing the magnetizing current expression (A3) derived in the Appendix, which can be rewritten as

$$i_M = 2C_{S2}\left|\frac{dv_{S2}}{dt}\right| + C_{OSS}\frac{dv_{DS}}{dt}, \qquad (9)$$

because voltage change dv_{S2}/dt is negative. To maintain the volt-second balance of the transformer as duty cycle D increases and the reset time decreases, the slope of negative reset voltage v_1 during turn-off time of switch Q_1 must increase. This requires higher dv/dt rates of voltages v_{DS} and v_{S2}. Therefore, as duty cycle D increases both current $i_{COSS} = C_{OSS}dv_{DS}/dt$ and $i_2 = C_{S2}|dv_{S2}/dt|$ increase, leading to the increase of magnetizing current i_M. For a given duty cycle, i.e., constant dv/dt rates of v_{DS} and v_{S2}, the magnetizing current is directly proportional to the string and switch

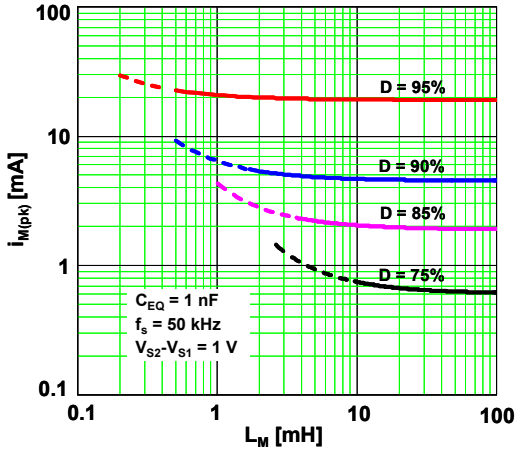

Fig. 7. Plot of peak magnetizing current $i_{M(pk)}$ vs. magnetizing inductance L_M.

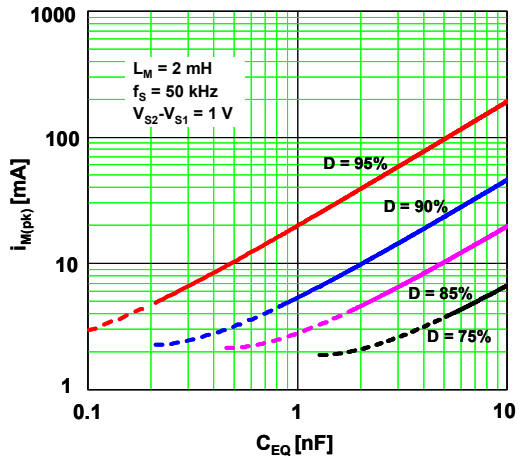

Fig. 8. Plot of peak magnetizing current $i_{M(pk)}$ vs. equivalent capacitance C_{EQ}.

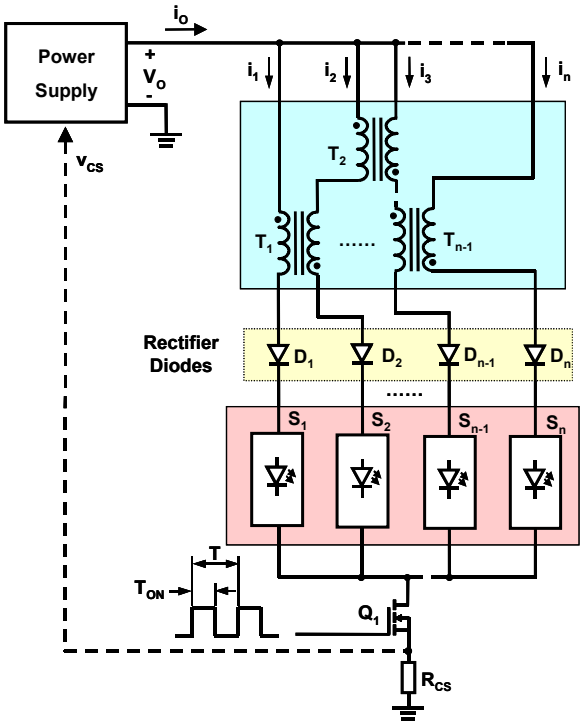

Fig. 9. Improved current balancer with low-capacitance rectifier diode in series with each LED string.

capacitances. To reduce i_M, capacitance of the switch and LED-string capacitances need to be minimized. Generally, the LED-string capacitance is reduced by connecting more LEDs in a string. In strings with a small number of LEDs, the equivalent string capacitance can be reduced by adding a low-capacitance rectifier diode (not an LED) in series with the LED string, as shown in Fig. 9.

The increase of the current-balancing error with increasing frequency, shown in Fig. 10, can also be attributed to the increased dv_{DS}/dt and dv_{S2}/dt rates. Namely, as the switching

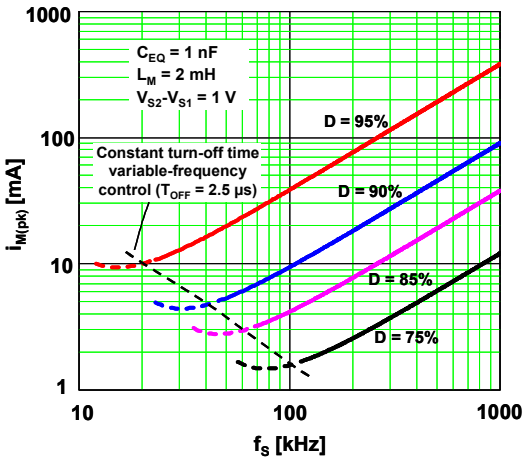

Fig. 10. Plot of peak magnetizing current $i_{M(pk)}$ vs. switching frequency f_S.

frequency increases, the available reset time of the transformer decreases, which produces higher dv/dt rates and, consequently, increases the magnetizing current. Therefore, the selection of the switching frequency is based on the trade-off between the size of the transformer and current-balancing accuracy.

Although the primary function of the switch(es) in series with LED strings is to provide the reset of the magnetic cores of current-balancing transformers, the switch(es) can also be used to provide PWM dimming. Namely, because the light intensity of LEDs is proportional to the average current, the light intensity can be controlled by changing the duty-cycle of the switch. This high-frequency PWM dimming can be implemented either by constant- or variable-frequency control, or by a combination of these two methods. In the PWM dimming control with the constant-off time and variable-frequency, the light intensity decreases as the dimming frequency increases, whereas, with the constant on-time variable-frequency dimming control the light intensity increases as the dimming frequency increases. As illustrated by the dashed line in Fig. 10, the current balancing error can be minimized by employing the constant-off-time variable-frequency control, i.e., by operating at the minimum frequency with maximum brightness (maximum duty cycle) and by increasing the frequency to achieve dimming.

The proposed LED driver can also be implemented with the conventional low-frequency dimming control, where a low-frequency signal (typically in the 200-500 Hz range) is used for dimming. In this case, the dimming signal applied to the switch(es) is obtained by combining a high-frequency drive signal of the switch(es) with a low-frequency dimming signal having a duty cycle D_{LF} through an "AND" logic circuit. By varying D_{LF}, the average current and, therefore, the brightness of each LED string can be adjusted.

V. Experimental Results

The performance of the proposed current balancer was experimentally verified with paralleled high-brightness LED

strings, built with LXHL-LM3C HB LEDs from Philips Lumileds, with a nominal string-current amplitude of I_{NOM} = 350 mA. A MOSFET (PHT4NQ10T from NXP) was used as the control switch. Figure 11 shows the measured relative current mismatch (error) ERR = $(\Delta I_{LED}/I_{NOM})\cdot 100\%$ as a function of the duty cycle for two severely mismatched LED strings, one with seven and the other with eight LEDs in series, without and with the proposed current balancer operating at 25 kHz. As can be seen, without a current balancing circuit, the current mismatch is approximately 100%, and virtually independent of the duty cycle. The proposed current balancer reduces this mismatch to below 10% in the entire duty-cycle range. Typical LED-string current waveforms without and with the proposed current balancer are shown in Fig. 12 with D = 85%.

The measured dependence of the relative current mismatch of the two strings on the switching frequency is shown in Fig.13. As can be seen from Fig. 13 (a), for large duty cycles, the current mismatch increases as the frequency increases. For example, for D = 95%, the current mismatch increases from 10% to 40% as the frequency is increased from 25 kHz to 100 kHz, which is in good agreement with the predicted behavior shown in the plot in Fig. 10. The current mismatch can be decreased by adding a low-capacitance rectifier diode in series with each LED string as shown in Fig. 9. As illustrated in Fig. 13 (b), the measured current mismatch of the two strings with the rectifier diodes added was reduced to the 5-20% range for D = 95%, depending on the switching frequency.

Figure 14 shows the effect of the rectifier diodes on the current balancing performance of two paralleled mismatched strings with various numbers of LEDs. Comparing the corresponding measurements without the rectifiers in Fig.14(a) and with the rectifiers in Fig.14(b), it can be seen that the effect of the rectifier diodes is more pronounced in the strings with a fewer number of LEDs since the string capacitance increases with decreasing number of LEDs in series. Moreover, from Fig.14(b) it can be seen that by adding the rectifier diodes, the current mismatch becomes virtually independent of the number of LEDs in the strings. For example, for D = 95%, the current mismatch of the two strings is lower than 10% regardless of the number of LEDs in the strings because the string capacitance is primarily determined by the capacitance of the rectifier diode.

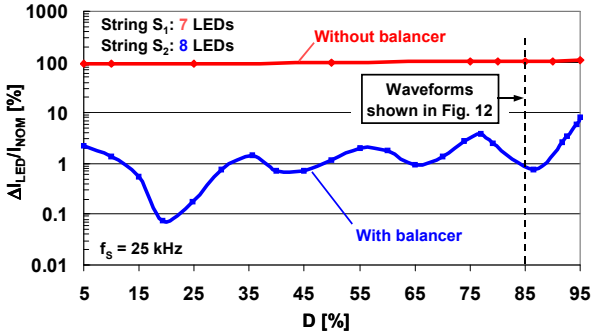

Fig. 11. Plot of relative current mismatch vs. duty cycle for two LED strings with/without current balancer.

Figure 15 shows the measured comparison of the current balancing performance between the constant-frequency control and constant-off-time variable-frequency control. The constant-frequency control was implemented with switching frequency f_S = 100 kHz, whereas the off-time of the variable-frequency control was set to T_{OFF} = 2.5 µs so that with D=95% the circuit was operating with switching frequency f_S =20 kHz, which is above the audible range. As can be seen from Fig. 15, with such a selection of T_{OFF}, the switching frequency of 100kHz is reached at D = 75%. To avoid operation at excessively high frequencies, the frequency was limited to 100 kHz, i.e., for duty cycles lower than D = 75% (not shown in Fig. 15), the constant-frequency control was used. As can be seen from the figure, with the constant-off-time control, current balancing better than 2% can be achieved in the entire dimming duty-cycle range.

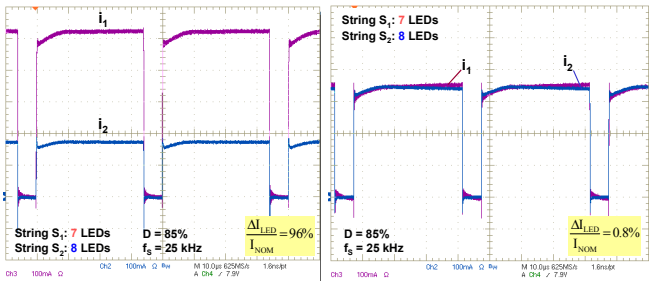

Fig. 12. Measured current waveforms of two LED strings: (a) without current balancing circuit; (b) with proposed current balancer.

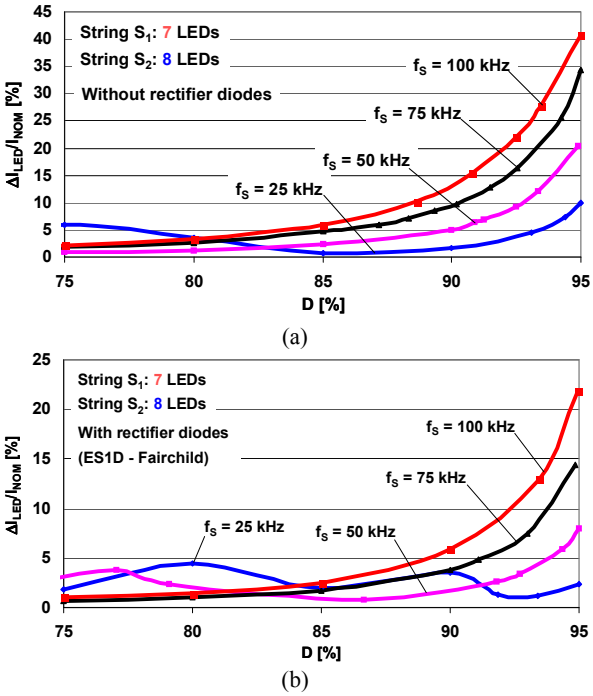

Fig. 13. Plot of relative current mismatch vs. duty cycle for different constant switching frequencies: (a) without series rectifier diodes; (b) with series rectifier diodes.

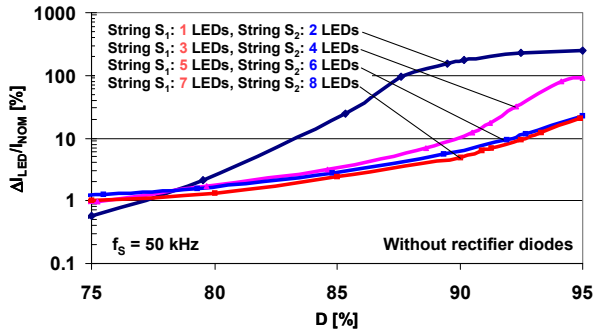

(a)

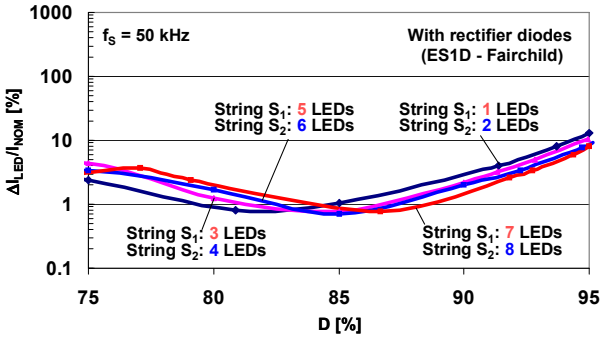

(b)

Fig. 14. Plot of relative current mismatch vs. duty cycle for different combinations of LEDs: (a) without series rectifier diodes; (b) with series rectifier diodes.

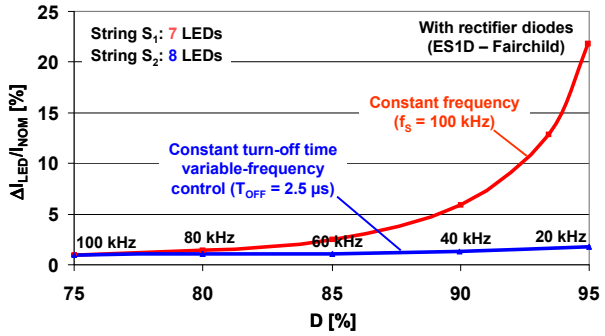

Fig. 15. Plot of relative current mismatch vs. duty cycle with different controls.

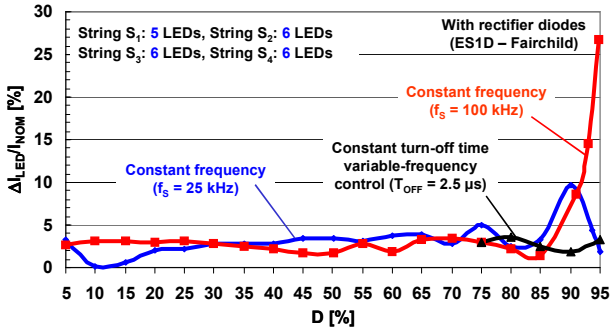

Fig. 16. Plot of relative current mismatch vs. duty cycle for four paralleled LED strings with series rectifier diodes.

Finally, Fig. 16 shows the measurement results for four strings in parallel, where three strings are composed of six LEDs and the fourth string of five LEDs in series. Even with four severely mismatched strings, a current balancing better than 4% can be achieved with a combination of the constant-off-time variable-frequency control (D: 75%~95%, f_S: 100 kHz ~ 20 kHz) and constant-frequency control (D: 5%~75%, f_S: 100 kHz).

VI. Summary

A low-cost, dc-input driver for paralleled LED strings with current balancing and dimming capabilities is proposed. The current balancing is implemented by operating the current balancing transformers at high frequencies. By modulating the duty cycle of the high-frequency switching, a wide-range dimming of the paralleled LED strings can also be achieved. The dimming control can be implemented either by the constant- or variable-frequency control, or by their combination. It was experimentally demonstrated that with the combined control a current balancing better than 4% can be achieved in the entire dimming range. Since the proposed current balancer is not integrated with the power supply (source) it can be used with any dc power source.

References

[1] M. Doshi and R. Zane, "Digital architecture for driving large LED arrays with dynamic bus voltage regulation and phase shifted PWM," IEEE Applied Power Electronics Conference (APEC) Proc., pp. 287 - 293, Feb. 2007.

[2] C. H. Lin, T. Y. Hung, C. M. Wang, and K. J. Pai, "A balancing strategy and implementation of current equalizer for high power LED backlighting," 7th International Conference on Power Electronics and Drive Systems (PEDS'07), pp. 1613 – 1617, Nov. 2007.

[3] C. L. Chiu and K. H. Chen, "A high accuracy current-balanced control technique for LED backlight," Power Electronics Specialists Conference (PESC'08), pp. 4202 – 4206, June 2008.

[4] C. Y. Wu, T. F. Wu, J. R. Tsai, Y. M. Chen, and C. C. Chen, "Multistring LED backlight driving system for LCD panels with color sequential display and area control," IEEE Transactions on Industrial Electronics, vol.55, no.10, pp.3791-3800, Oct. 2008.

[5] Y. Hu and M. M. Jovanovic, "LED driver with self-adaptive drive voltage," IEEE Transactions on Power Electronics, vol. 23, no. 6, pp. 3116-3125, Nov. 2008.

[6] E. C. Kang, D. Kwon, J. E. Yeon, D. S. Kim and W. Oh, "A new low voltage detecting method for multi-string LED BLU circuit," European Conference on Power Electronics and Applications (EPE '09), Sept. 8-10, 2009.

[7] H. J. Chiu, Y. K. Lo, J. T. Chen, S. J. Cheng, C. Y. Lin, and S. C. Mou, "A high-efficiency dimmable LED driver for low-power lighting applications," IEEE Transactions on Industrial Electronics, vol.57, no.2, pp.735-743, Feb. 2010.

[8] M. Doshi and R. Zane, "Control of solid-state lamps using a multiphase pulsewidth modulation technique," IEEE Transactions on Power Electronics, vol.25, no.7, pp.1894-1904, July 2010.

[9] S. M. Baddela and D. S. Zinger, "Parallel connected LEDs operated at high frequency to improve current sharing," Proc. IEEE IAS'04, pp. 1677-1681, 2004.

[10] C.C. Chen, C. Y. Wu, and T. F. Wu, "Fast transition current-type burst-mode dimming control for the LED backlight driving system of LCD TV," IEEE Power Electronics Specialists Conference (PESC) Proc., pp. 1- 7, June 18-22, 2006.

[11] W. Thomas and J. Pforr, "A novel low-cost current-sharing method for automotive LED-lighting systems," 13th European Conference on Power Electronics and Applications (EPE '09), Sept. 8-10, 2009.
[12] K. I. Hwu and Y. T. Yau, "Applying one-comparator counter-based sampling to current sharing control of multi-channel LED strings," IEEE Applied Power Electronics Conference (APEC) Proc., pp. 737-742, Feb. 21-25, 2010.
[13] S. Choi, P. Agarwal, T. Kim, J. Yang, and B. Han, "Symmetric current balancing circuit for multiple DC loads," IEEE Applied Power Electronics Conference (APEC) Proc., pp. 512 - 518, Feb. 21-25, 2010.
[14] C. T. Huang, S. J. Yan, C. C. Cheng, and P. Y. Lee, "Power supply circuit with current sharing for driving multiple sets of dc loads," US Pat. Appl. No. 2009/0195169, Aug. 6, 2010.
[15] S. S. Hong, S. H. Lee, S. H. Cho, C. W. Roh, and S. K. Han, "A new cost-effective current-balancing multi-channel LED driver for a large screen LCD backlight units," Journal of Power Electronics, vol. 10, no. 4, pp.351-356, 2010.
[16] K. I. Hwu, and S. C. Chou, "A simple current-balancing converter for LED lighting," IEEE Applied Power Electronics Conference (APEC) Proc., pp. 587 - 590, Feb. 2009.
[17] X. Jin, "Balancing transformers for ring balancer," US Pat. 7,294971, Nov. 13, 2007.
[18] C. D. Wey, Y. Y. Yu, H. J. Li and Y. P, Lee, "Balanced circuit for multi-LED driver," US Pat. 7,358,684, April 15, 2008.

APPENDIX

DERIVATION OF MAGNETIZING CURRENT EXPRESSION

In the most general case, the magnetizing current of the current-balancing transformer in the proposed driver has the waveform shown in Fig. A1. The shown waveform represents a continuous magnetizing current with minimums (valleys) $i_{M(min)}$ occurring at the end of the switching cycles.

To simplify the derivation, it is assumed that the duration of the stage in Fig. 6(b) is very short in comparison with the switching period, i.e., it is assumed that the increase of the magnetizing current after the switch is turned off is small compared to the peak current magnitude. This assumption implies that equivalent series resistance R_S of the string is small so that the voltage drop across it produced by the string current is negligible. Since this assumption is reasonable in the majority of practical circuits, neglecting the stage in Fig. 6(b) has no significant effect on the accuracy of these derivations. With this assumption, the peak magnetizing current can be approximated with

$$i_{M(pk)} \cong i_{M(min)} + \Delta i_M , \qquad (A1)$$

where Δi_M is given by (5) and $i_{M(min)}$ needs to be determined.

With reference to Fig. 6(c), it follows that

$$i_M - i_2 = i_{COSS} + i_2 , \qquad (A2)$$

which can be also expressed as

$$i_M + 2C_{S2}\frac{dv_{S2}}{dt} - C_{OSS}\frac{dv_{DS}}{dt} = 0 , \qquad (A3)$$

where

$$v_{S2} = v_1 + v_2 + V_{SI} = 2v + V_{SI} , \qquad (A4)$$

$$v_{DS} = V_O - v_1 - V_{SI} = V_O - v - V_{SI} , \qquad (A5)$$

and $v_1 = v_2 = v$ because of the unity turns ratio of the transformer.

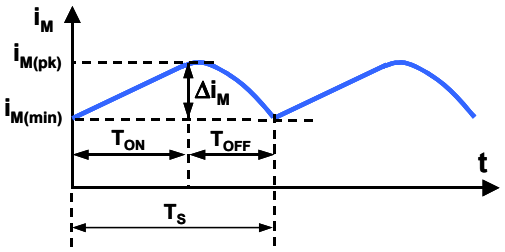

Fig. A1 Waveform of magnetizing current

Because V_O and V_{SI} are constant, (A3) can be rewritten as

$$i_M + 4C_{S2}\frac{dv}{dt} + C_{OSS}\frac{dv}{dt} = 0 . \qquad (A6)$$

By eliminating v from (A6) using

$$v = L_M\frac{di_M}{dt} , \qquad (A7)$$

one obtains

$$\frac{d^2 i_M}{dt^2} + K^2 i_M = 0 , \qquad (A8)$$

where

$$K = \frac{1}{\sqrt{L_M(4C_{S2} + C_{OSS})}} = \frac{1}{\sqrt{L_M C_{EQ}}} . \qquad (A9)$$

Since at the beginning of the off time of switch Q_1

$$i_M(t=0) = i_{M(min)} + \Delta i_M \qquad (A10)$$

and at the end of the off time of switch Q_1

$$i_M(t = T_{OFF}) = i_{M(min)} , \qquad (A11)$$

from the boundary-value solution of (A8), $i_{M(min)}$ is obtained as

$$i_{M(min)} = \frac{\cos(KT_{OFF})}{1 - \cos(KT_{OFF})}\Delta i_M . \qquad (A12)$$

Finally, from (A1), (5), (A9), and substituting T_{OFF} with $(1\text{-}D)/f_S$, the expression for the peak magnetizing current in (6) is obtained. This expression is valid as long as $i_{M(min)}>0$. Since $i_{M(min)}$ in (A12) equals zero when $KT_{OFF}=K(1\text{-}D)/f_S = \pi/2$, it follows that (6) is valid if

$$0 < \frac{K(1-D)}{f_S} \le \frac{\pi}{2} . \qquad (A13)$$

It should be noted that the validity range of (6) can be extended to

$$\frac{\pi}{2} < \frac{K(1-D)}{f_S} \le \pi , \qquad (A14)$$

with a reduced but still acceptable accuracy.